







## TEST REPORT

Ref: TR.106.2.08.SATL.C

# 0.8-12 GHz DUAL RIDGE HORN SATIMO TEST REPORT

### *Summary:*

This document summarizes the electrical and mechanical tests results performed for delivery acceptance by SATIMO for the Dual Ridge Horn SH800 covering the frequency range 0.8 – 12 GHz.

	<i>Name</i>	<i>Function</i>	<i>Date</i>	<i>Signature</i>
<i>Prepared by :</i>	B. BENCIVENGA L. SCIALACQUA	RF Engineer Antenna Engineer	2008/04/15	 
<i>Checked by :</i>	L. FOGED	Engineering Director	2008/04/15	
<i>Approved by :</i>	G. BARONE	Marketing Director	2008/04/15	

<i>Issue</i>	<i>Date</i>	<i>Modifications</i>
A	2008/04/15	Initial release
B	2009/04/23	Updated with phase center location and gain out of band.
C	2010/02/19	Updated gain out of band in the range [0.2-0.8]GHz

## TABLE OF CONTENTS

1	INTRODUCTION	4
2	MECHANICAL DESIGN	5
3	ELECTRICAL TESTING	7
4	RADIATIVE MEASUREMENTS	8
4.1	Typical Boresight Gain	9
4.2	Typical Efficiency	11
4.3	Phase Center Variation	12
4.4	Typical Dual Ridge Horn Angular 3dB Beamwidth	14
4.5	Directivity Pattern Cuts	15
5	TYPICAL AND MEASURED DATA ACCURACY	25
5.1	Return loss	25
5.2	Boresight Gain	25
5.3	Efficiency	25

## 1 INTRODUCTION

SATIMO Dual Ridge Horns combine stable gain performance and low VSWR with wide band frequency operation. The horns are single linearly polarized with excellent cross-polar discrimination, ideal as reference antennas for gain calibration of antenna measurement systems or as wideband probes in classical far field test ranges.

The unique horn design suppresses any possible excitation of higher order modes in the aperture and maintains a well defined smooth radiation pattern in the direction of the boresight axis throughout the operational bandwidth of the horn.

Thanks to the lightweight design in corrosion resistant aluminium and high reliability manufacturing technology, the horns are robust, low weight, easy to handle and have an excellent performance repeatability. The horns are equipped with a high precision female 3.5mm connector intermateable with SMA and K connectors, for superior repeatability and durability. The nominal impedance is 50 Ohm with return loss values better than  $-10$  dB ( $VSWR < 1.9$ ).

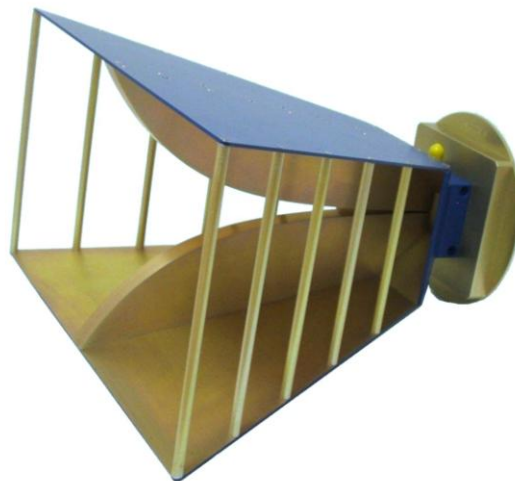


**Fig. 1-1:** *The SATIMO dual ridge 800MHz – 12 GHz horn.*

## 2 MECHANICAL DESIGN

The horn general features are listed in Table 2-1.

<b>Weight</b>	1.2 kg (approx)
<b>Overall dimensions</b> (H x W x L)	270 x 146.2 x 225 mm
<b>Connector</b>	H+S PC 3.5mm Female (Type 23 PC35-50-0-51/199 UE)

**Table 2-1:** *Horn general features.*

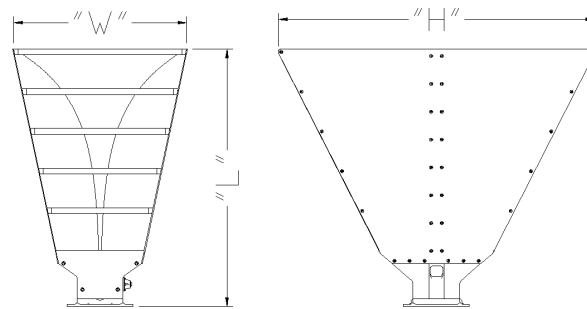


**Figure 2-1:** *Horn dimensions.*

A detailed mechanical drawing of the horn flange is shown in Figure 2-2.

The circular interface allows the user to center the antenna with very high accuracy. The horn is fastened to the customer's mounting support by four M5 screws and the alignment is determined by a precision pin in mechanical interface plate. The alignment accuracy is estimated in  $\pm 0.01^\circ$  on azimuth.

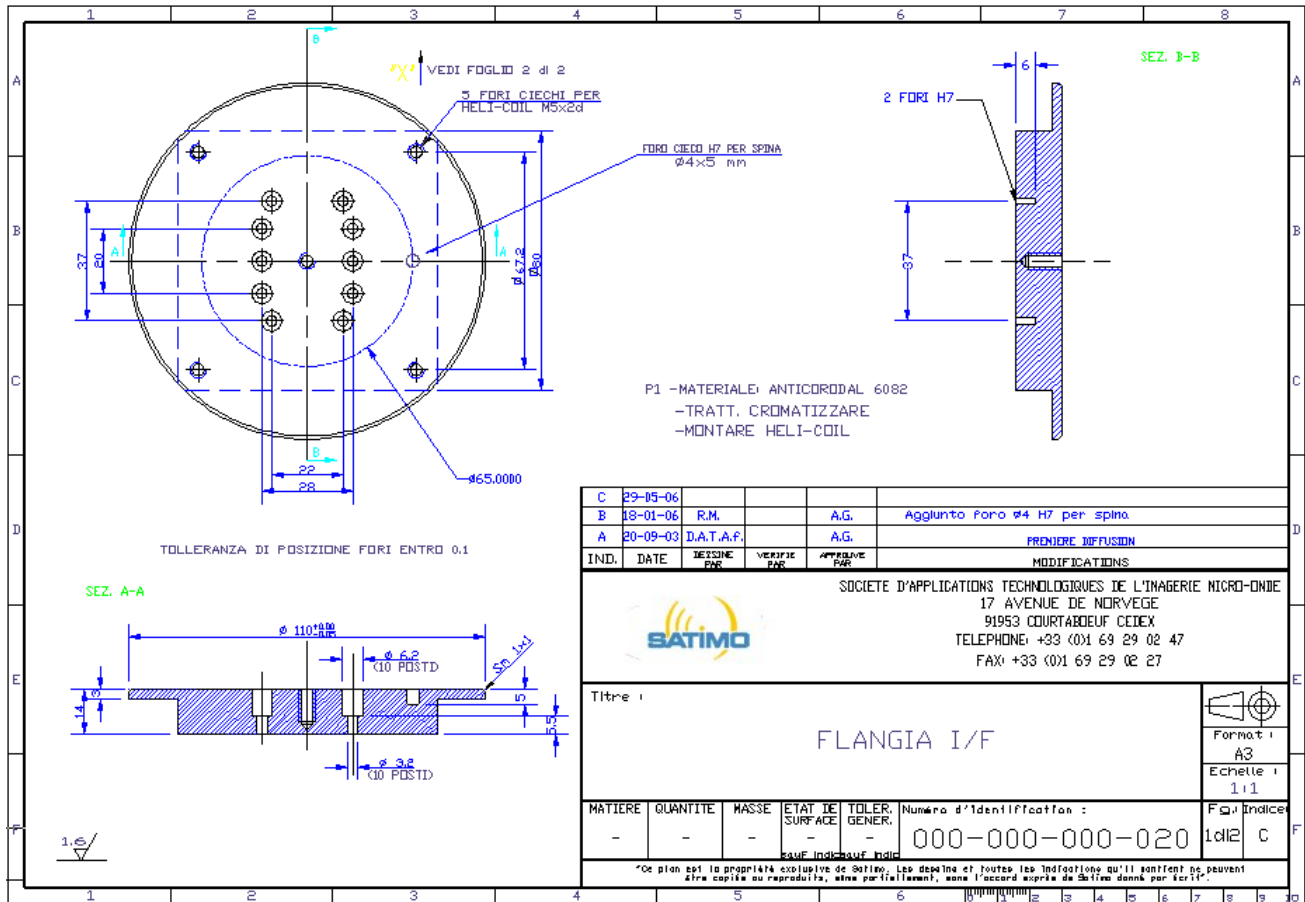
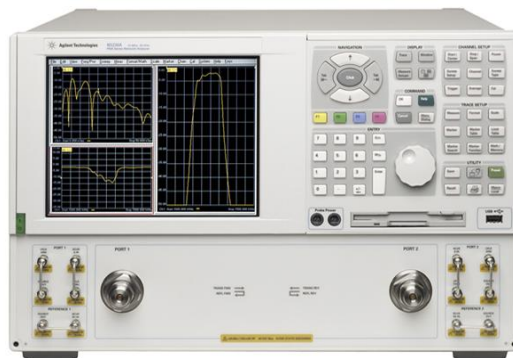


Figure 2-2: Mechanical drawing of the flange.

### 3 ELECTRICAL TESTING

The S11 performance has been measured with an Agilent PNA N5230A Vector Network Analyzer shown in Figure 3-1, calibrated with a Rosenberger calibration kit RPC-2.92.

The typical return loss with frequency is shown in Figure 3-2.



**Figure 3-1:** Agilent PNA N5230A Vector Network Analyzer.

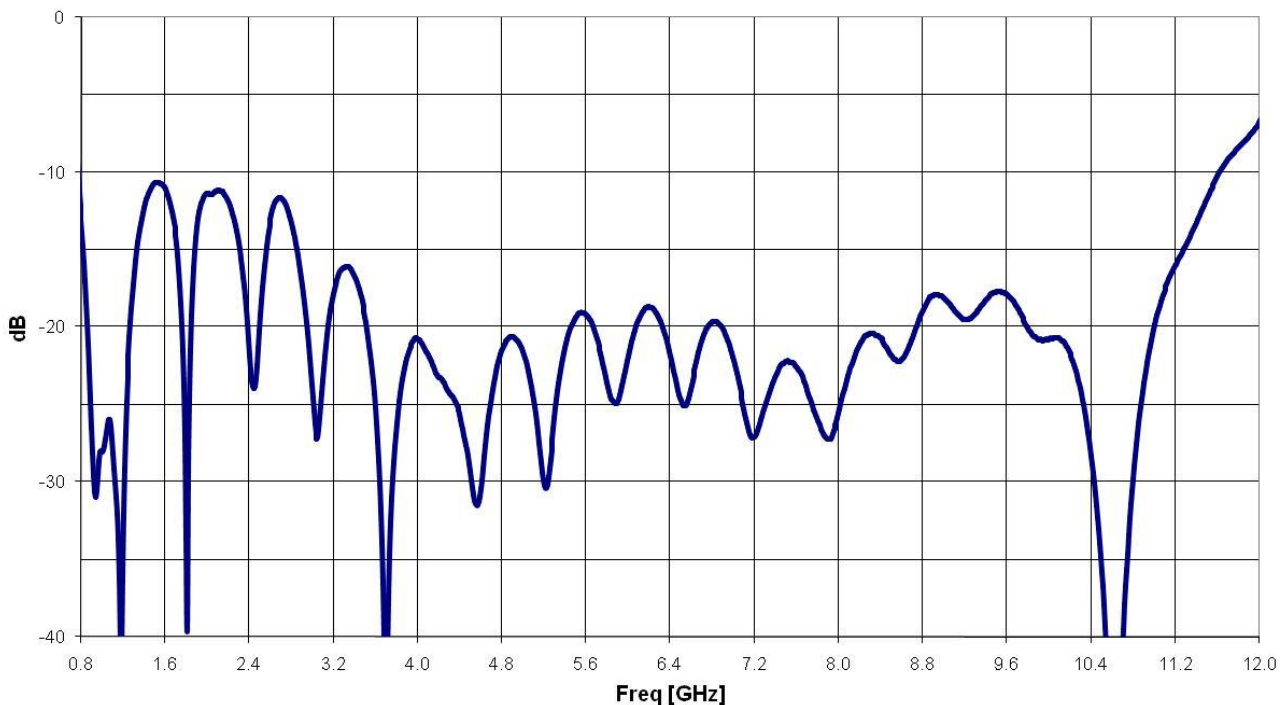


**Figure 3-2:** Typical return loss with frequency.

#### 4 RADIATIVE MEASUREMENTS

The radiated performances have been measured in the SATIMO Multi Probe spherical near field System (SG64) in USA, shown in Figure 4-1. The measurement set-up is shown in Figure 4-2.

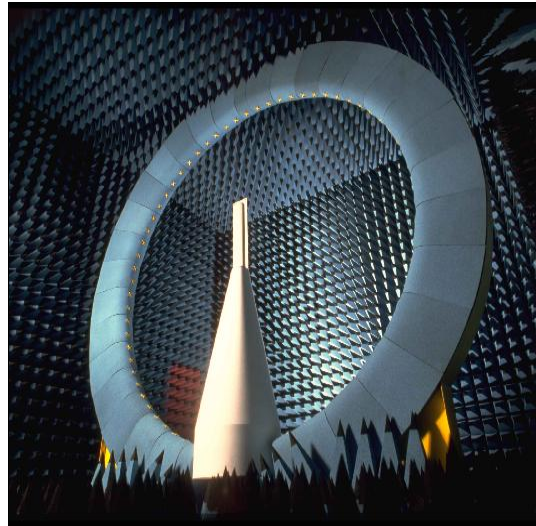


**Figure 4-1:** SATIMO Multi Probe spherical near field System (SG64) in USA.

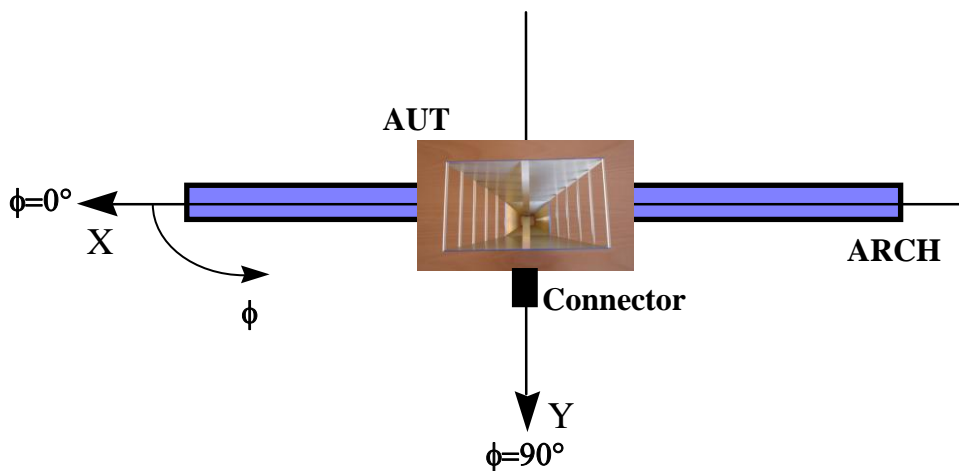


**Figure 4-2:** Measurement set-up.



#### 4.1 TYPICAL BORESIGHT GAIN

The typical boresight gain with frequency is shown in Figure 4-3. The reported antenna gain is  $4\pi$  times the ratio of the power radiated per unit solid angle in that direction to the net power delivered to the antenna by a  $50\Omega$  generator. This definition is also referred to as realized antenna gain which is less than the IEEE definition [IEEE Standard Test Procedures for Antennas, ANSI/IEEE Std 149-1979] by the value of the antenna return loss.

The boresight gain out of the frequency range is shown in Figure 4-4 and Figure 4-5.

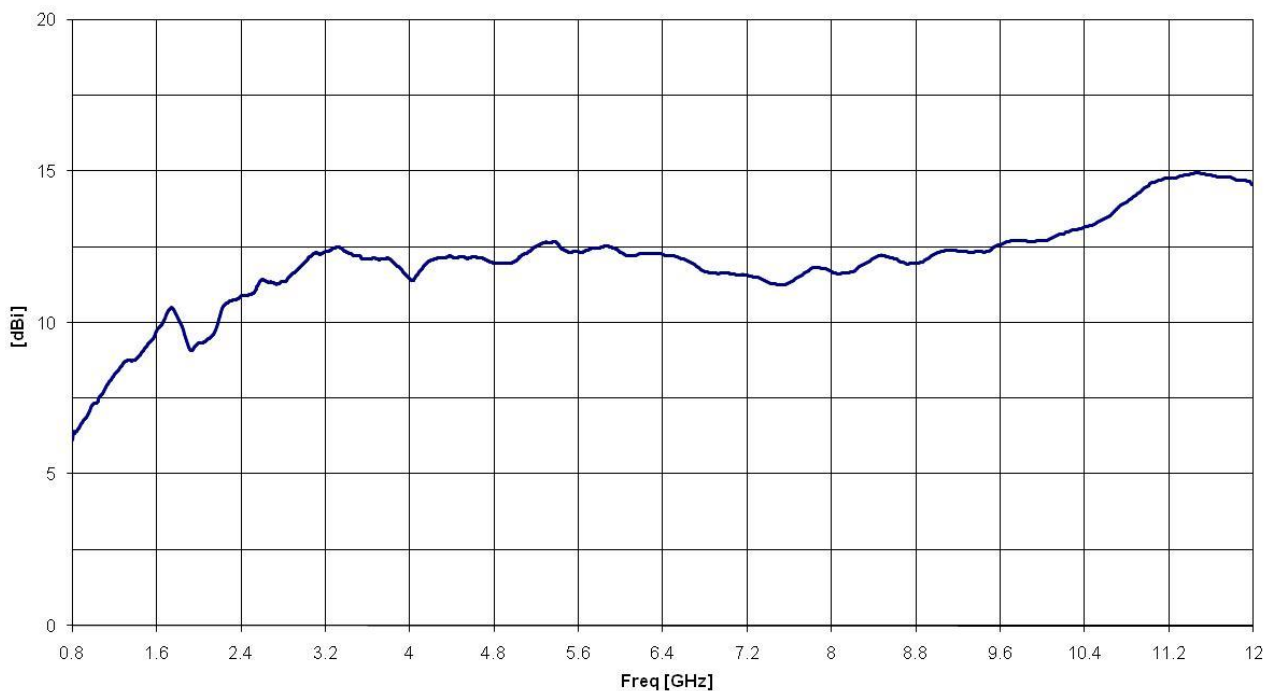


**Figure 4-3:** *Typical boresight gain with frequency.*

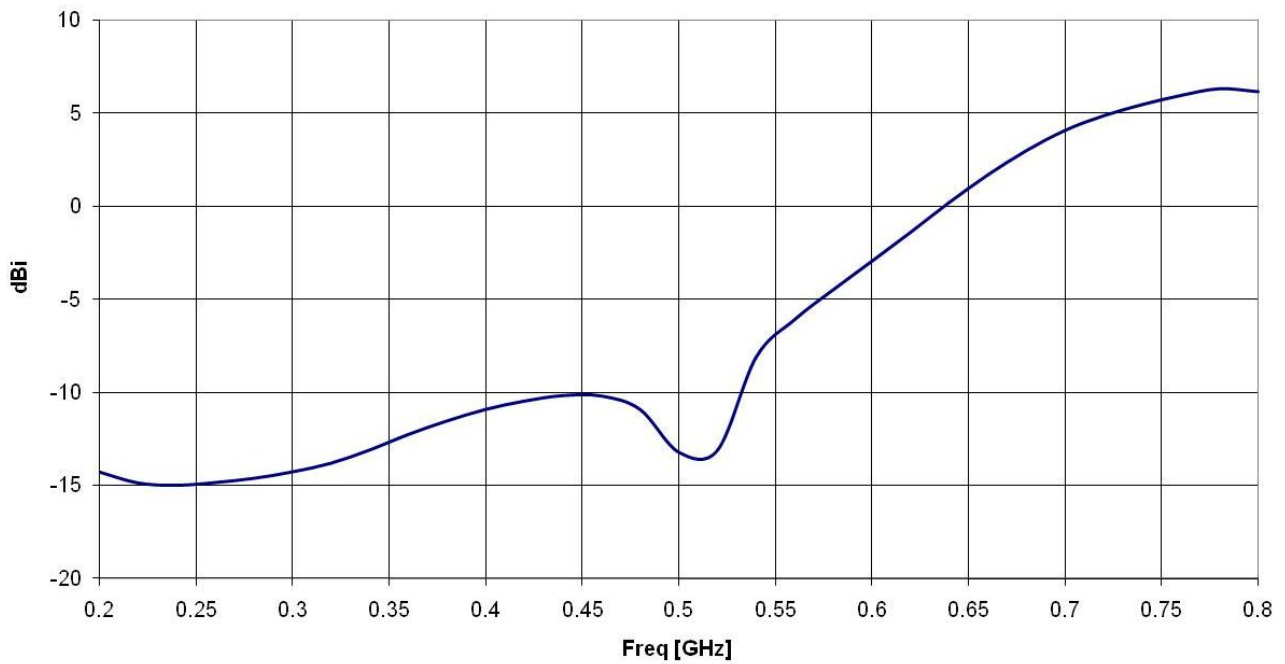


**Figure 4-4:** The boresight gain out of band [0.2-0.8]GHz.

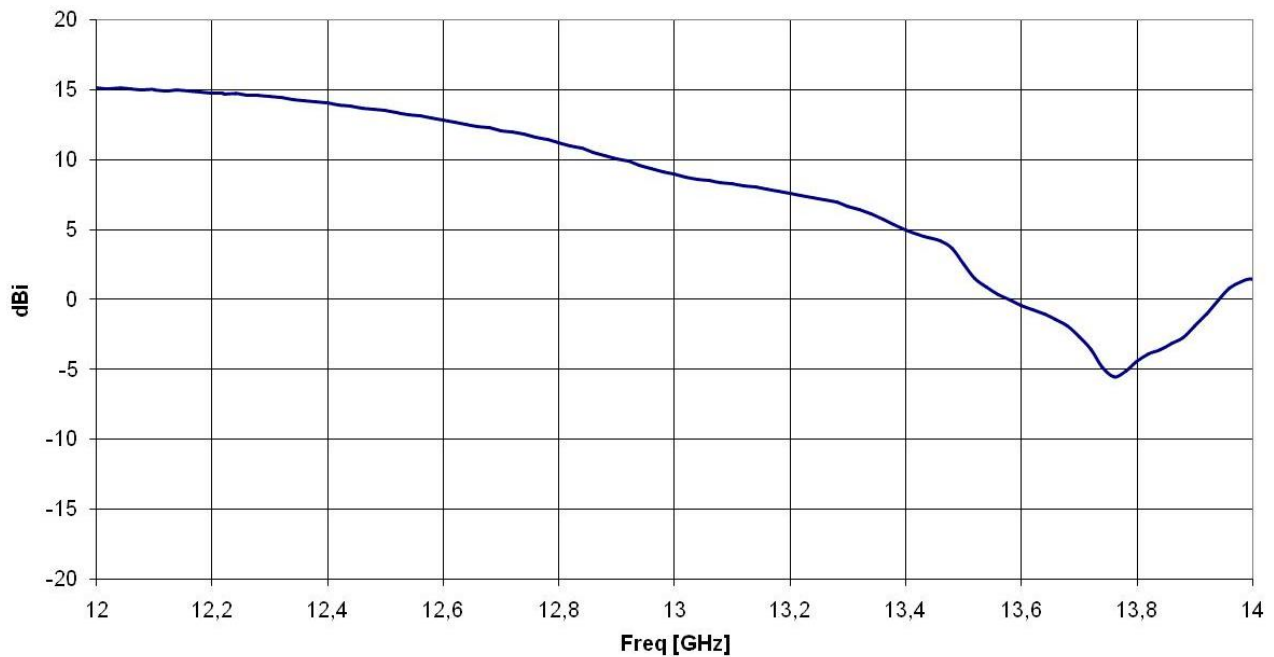


**Figure 4-5:** The boresight gain out of band [12-14]GHz.

## 4.2 TYPICAL EFFICIENCY

The typical efficiency with frequency is shown in Figure 4-6.

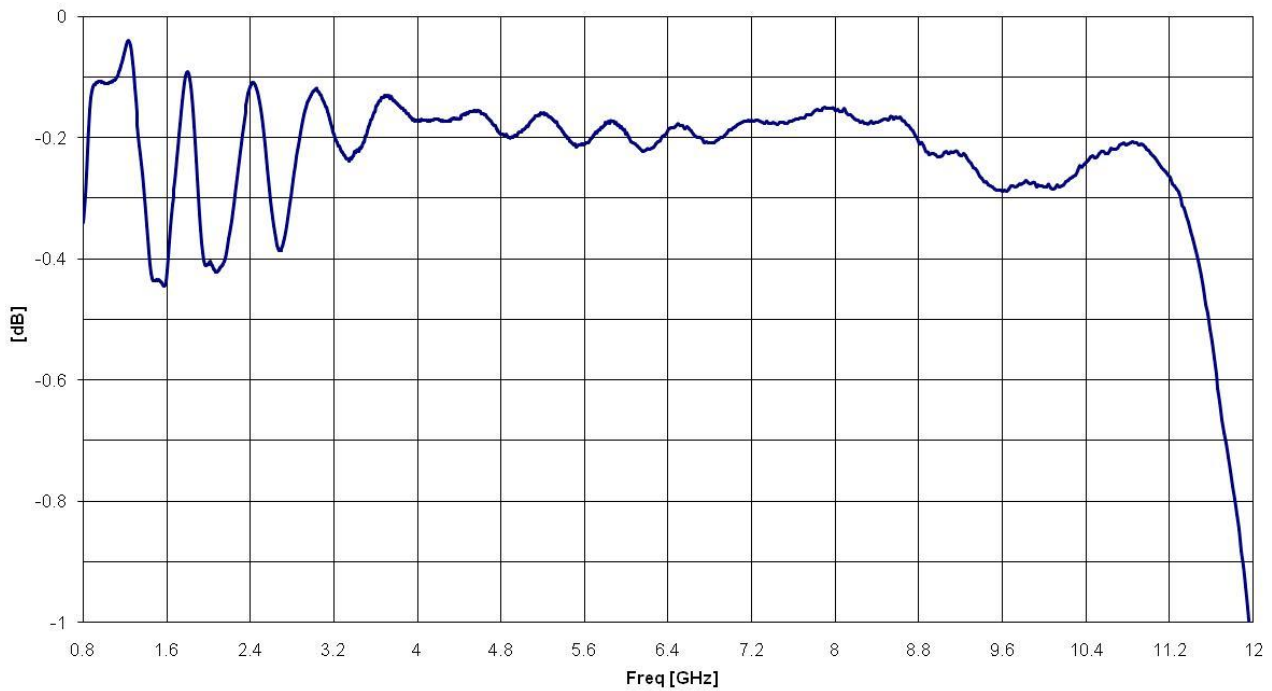


**Figure 4-6:** *Typical efficiency with frequency.*

### 4.3 PHASE CENTER VARIATION

Phase center variation with frequency (E and H plane) is shown in Figure 4-8 to Figure 4-10 for different elevation ranges  $[-\alpha, \alpha]$  deg.

The phase center plots ( $Z=0$ cm) are referred to the antenna aperture according to the reference system reported in Figure 4-7; a positive distance on the plot means that it is going inside the horn.

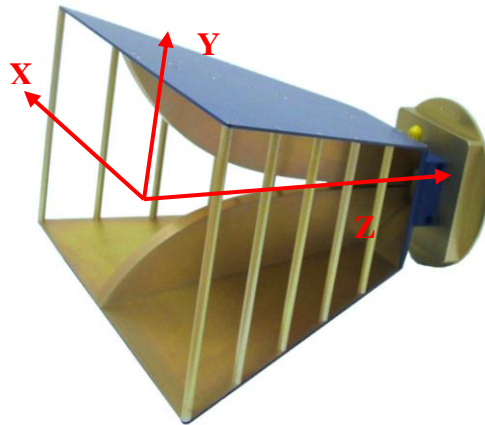


**Figure 4-7:** Phase center: reference coordinate system.

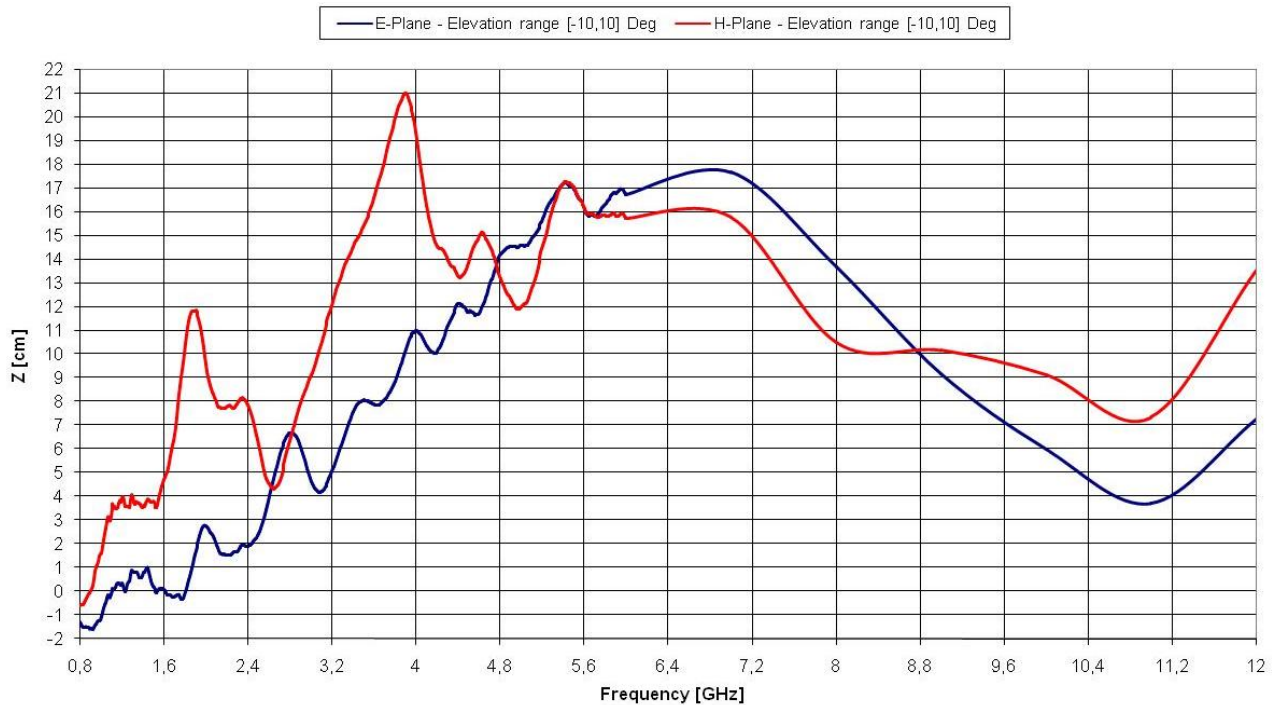


**Figure 4-8:** Phase Center Variation for elevation range  $[-10,10]$  deg  
( $z=0$ cm correspond to the aperture).

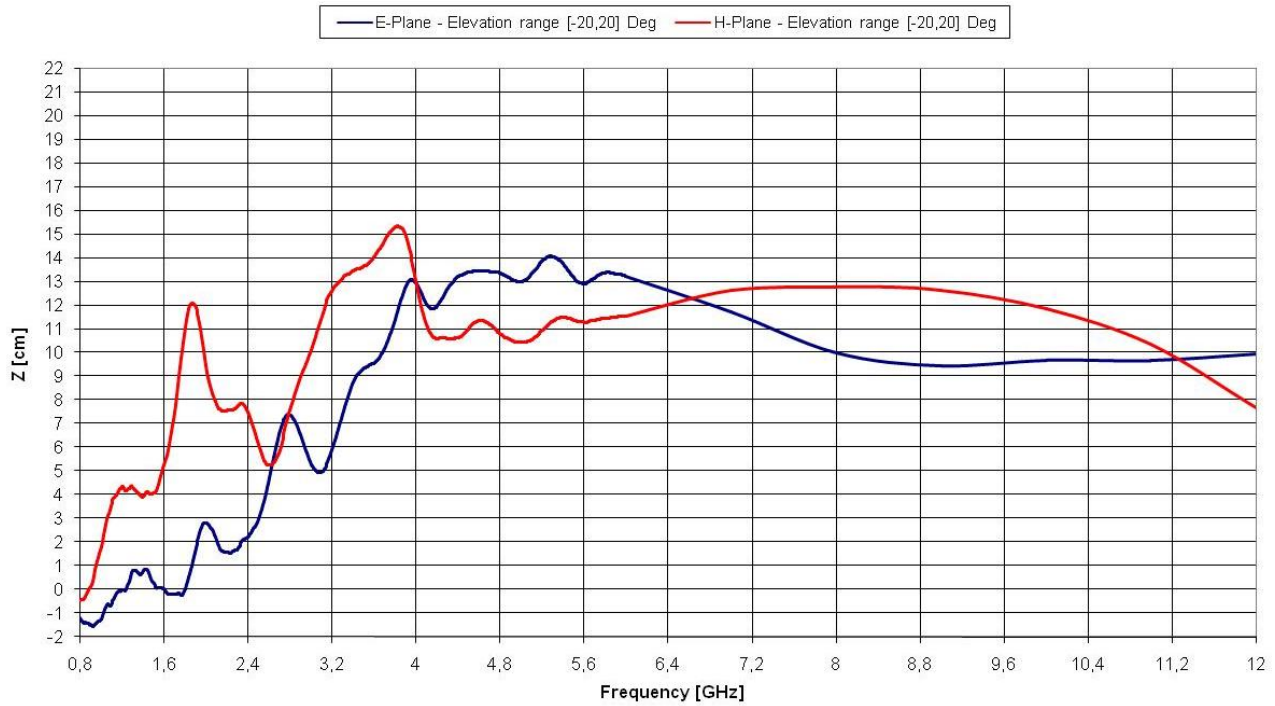


**Figure 4-9:** Phase Center Variation for elevation range [-20,20] deg  
( $z=0\text{cm}$  correspond to the aperture).

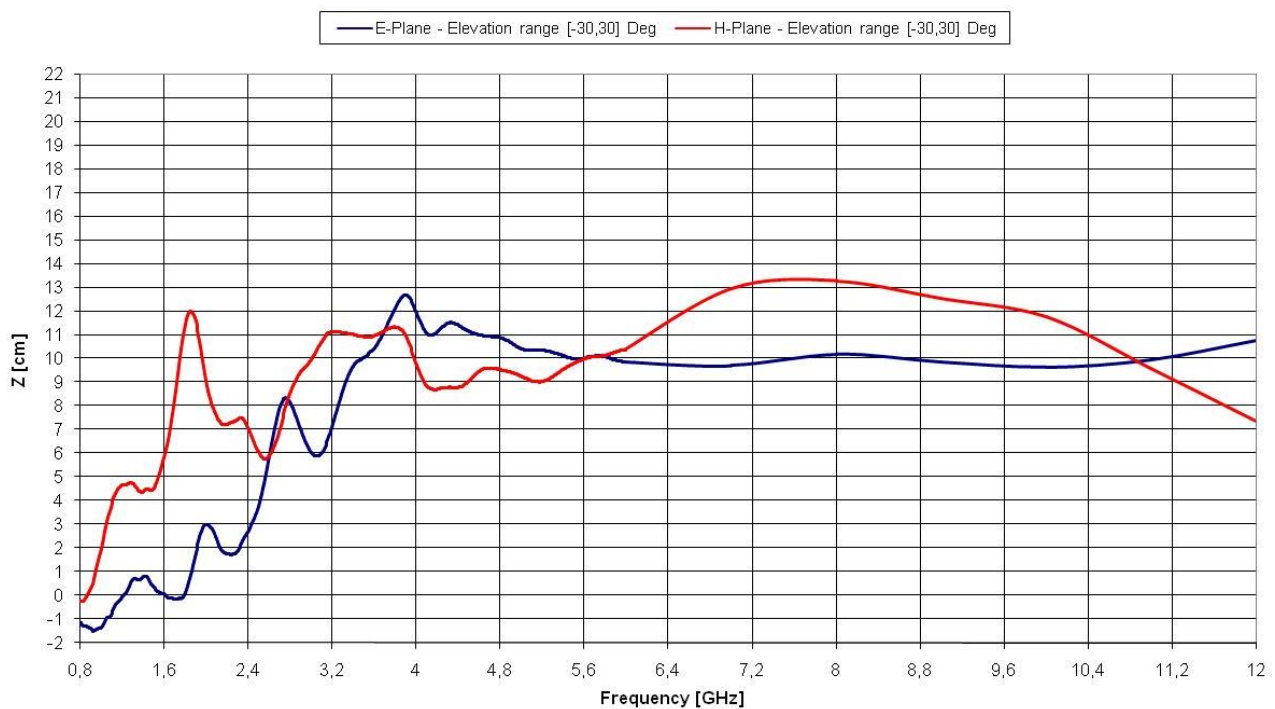


**Figure 4-10:** Phase Center Variation for elevation range [-30,30] deg  
( $z=0\text{cm}$  correspond to the aperture).

#### 4.4 TYPICAL DUAL RIDGE HORN ANGULAR 3DB BEAMWIDTH

The typical dual ridge horn angular 3dB beamwidth (2X) with frequency is shown in Figure 4-11.

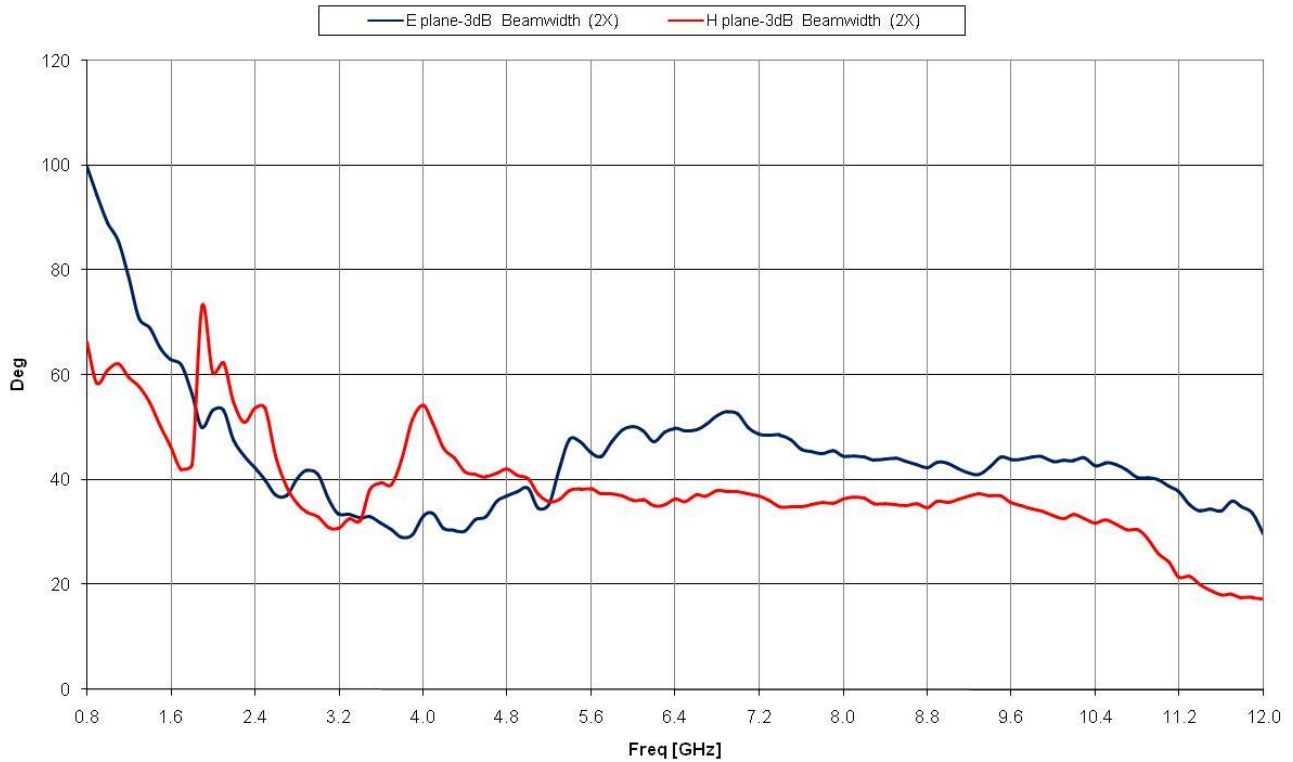


**Figure 4-11:** Typical dual ridge horn angular 3dB beamwidth (2X).

#### 4.5 DIRECTIVITY PATTERN CUTS

The typical directivity patterns cut with co-polar and cx-polar components (defined according to LudwigIII) from 0.824 GHz to 6 GHz are shown from Figure 4-12 to Figure 4-31.

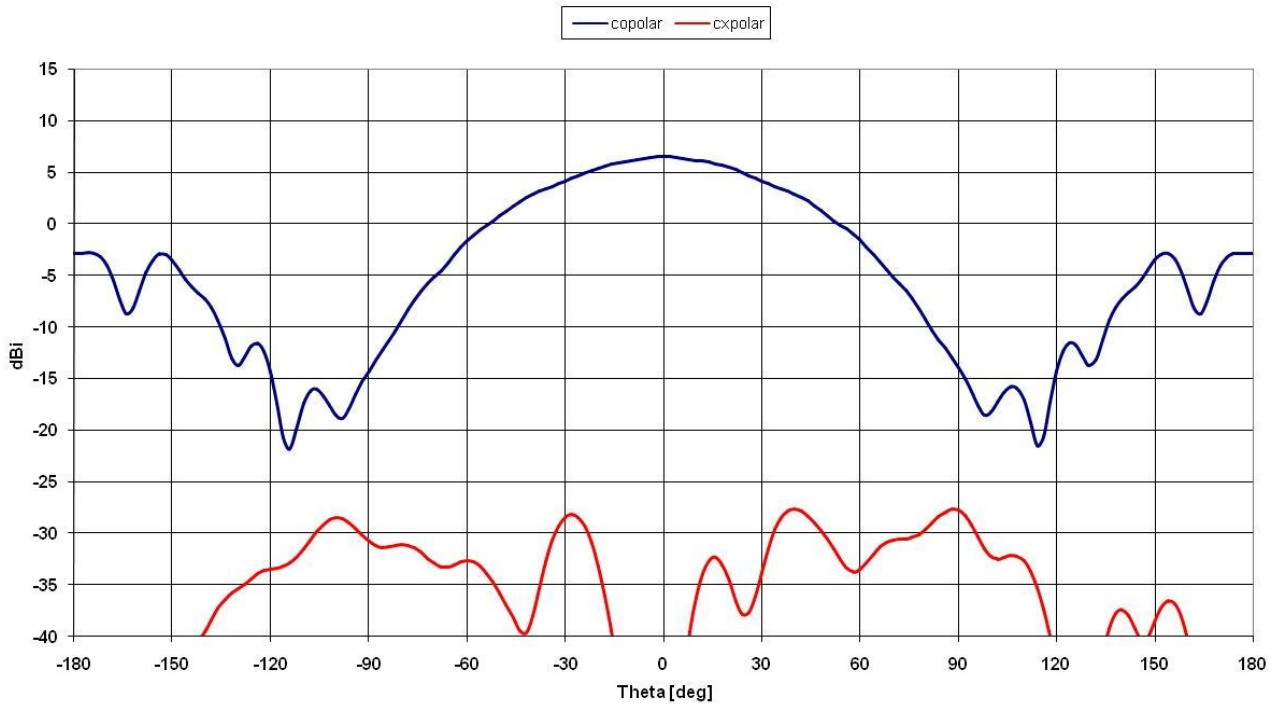


**Figure 4-12:** Directivity pattern @ 0.824 GHz,  $\phi=0^\circ$ .

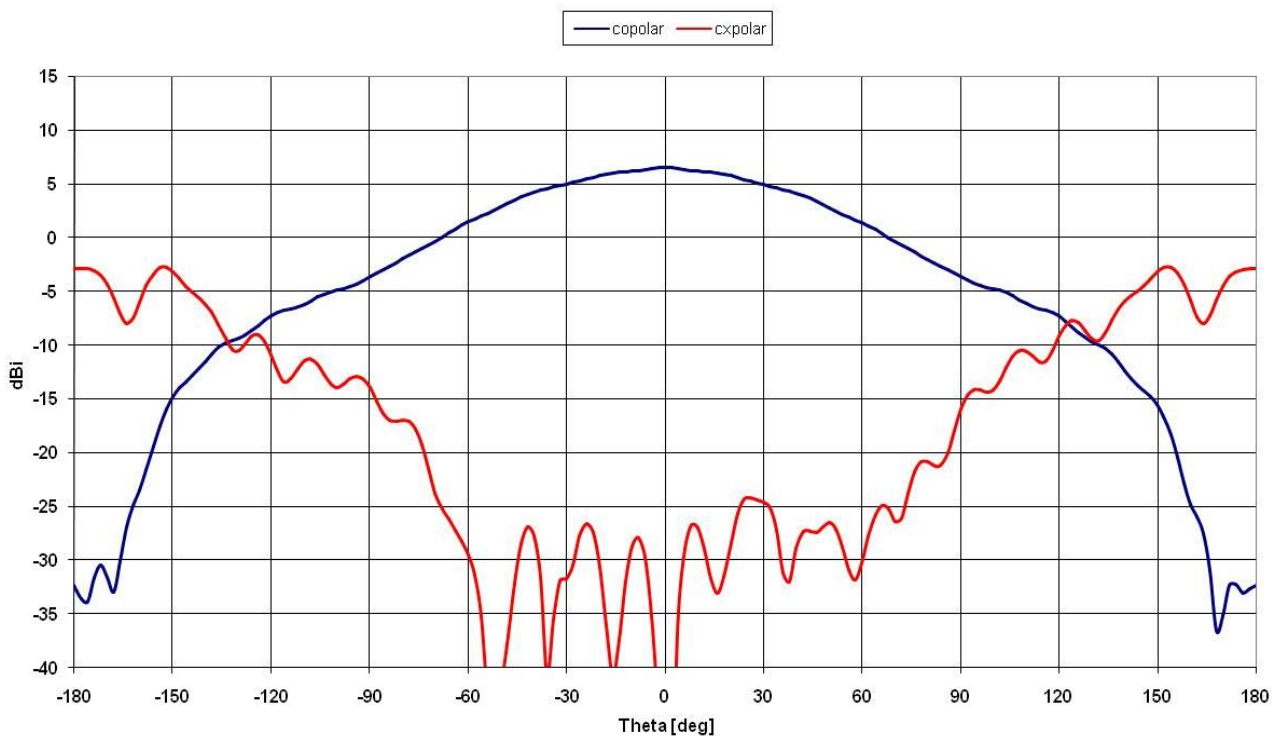


**Figure 4-13:** Directivity pattern @ 0.824 GHz,  $\phi=45^\circ$ .



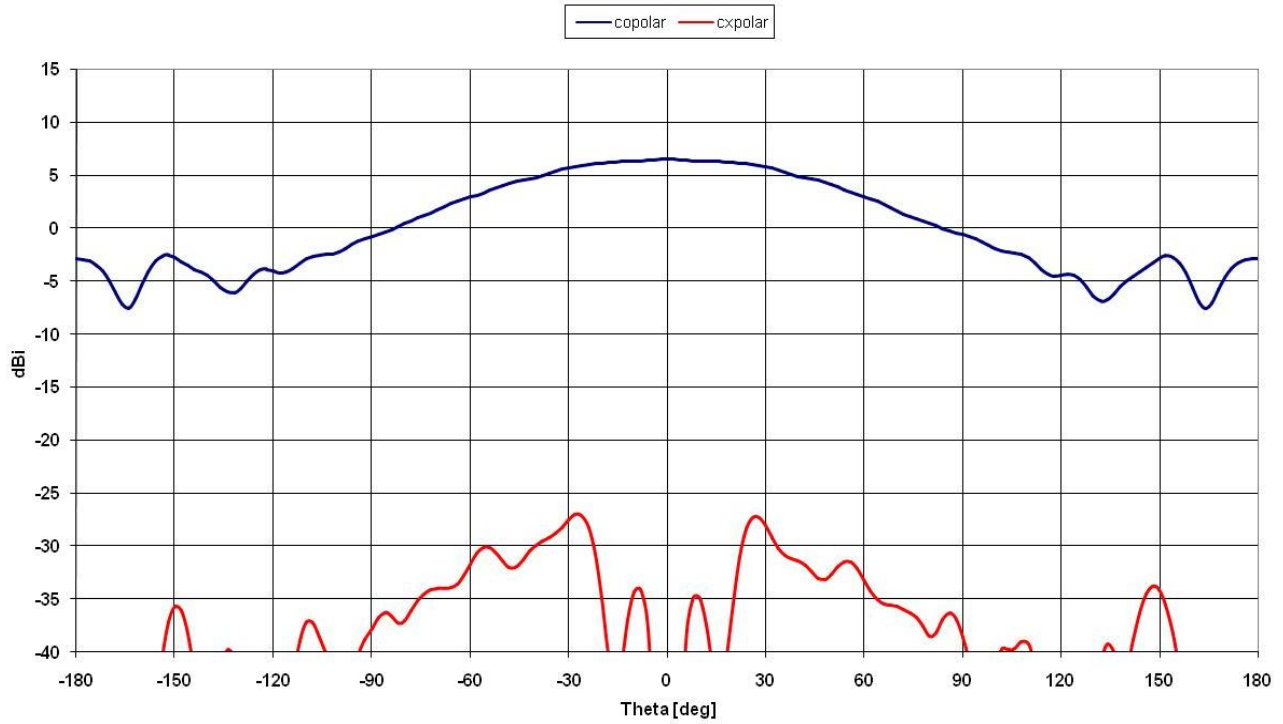


**Figure 4-14:** Directivity pattern @ 0.824 GHz,  $\phi = 90^\circ$ .

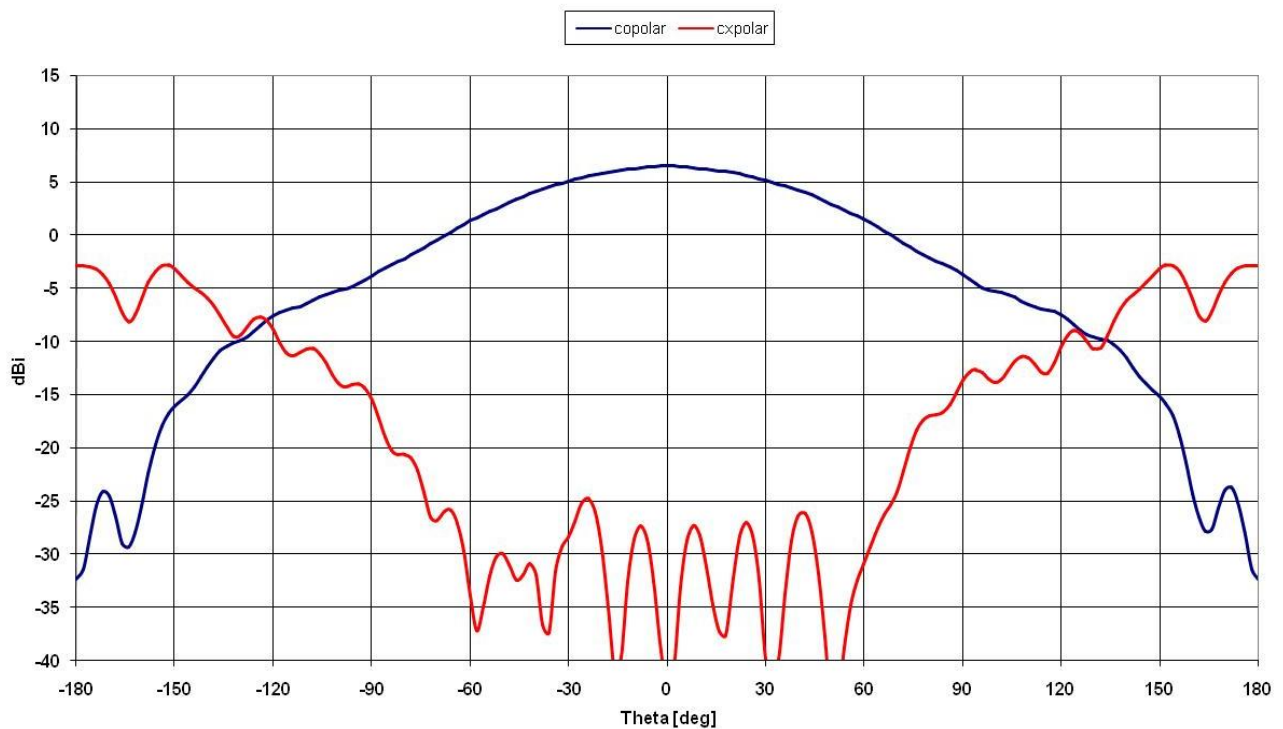


**Figure 4-15:** Directivity pattern @ 0.824 GHz,  $\phi = 135^\circ$ .



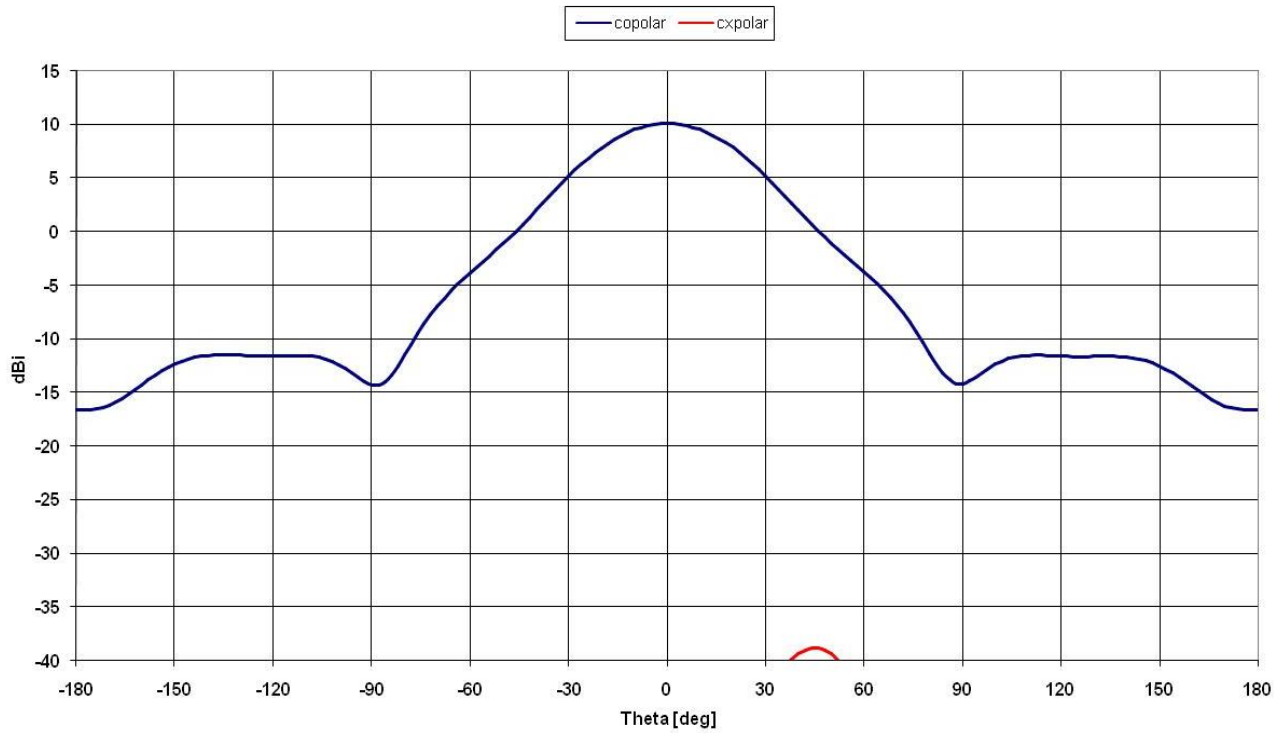


**Figure 4-16:** Directivity pattern @ 1.6 GHz,  $\phi=0^\circ$ .

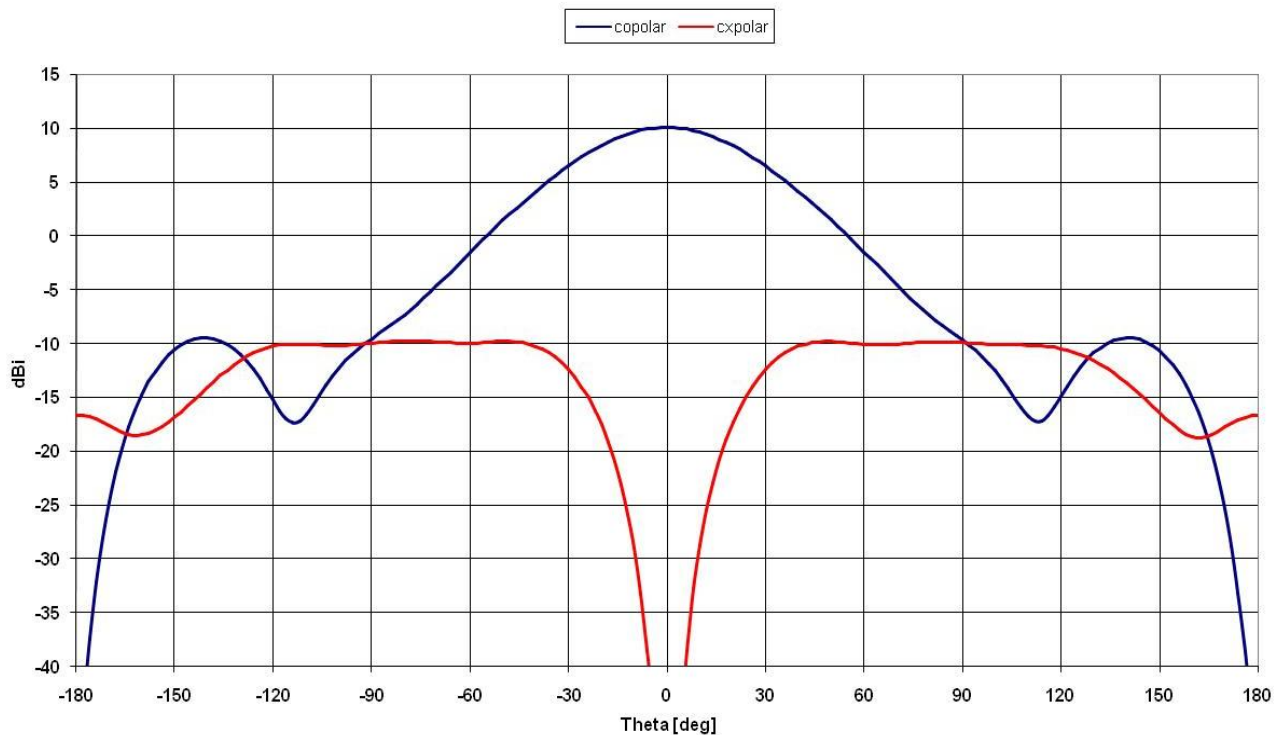


**Figure 4-17:** Directivity pattern @ 1.6 GHz,  $\phi=45^\circ$ .

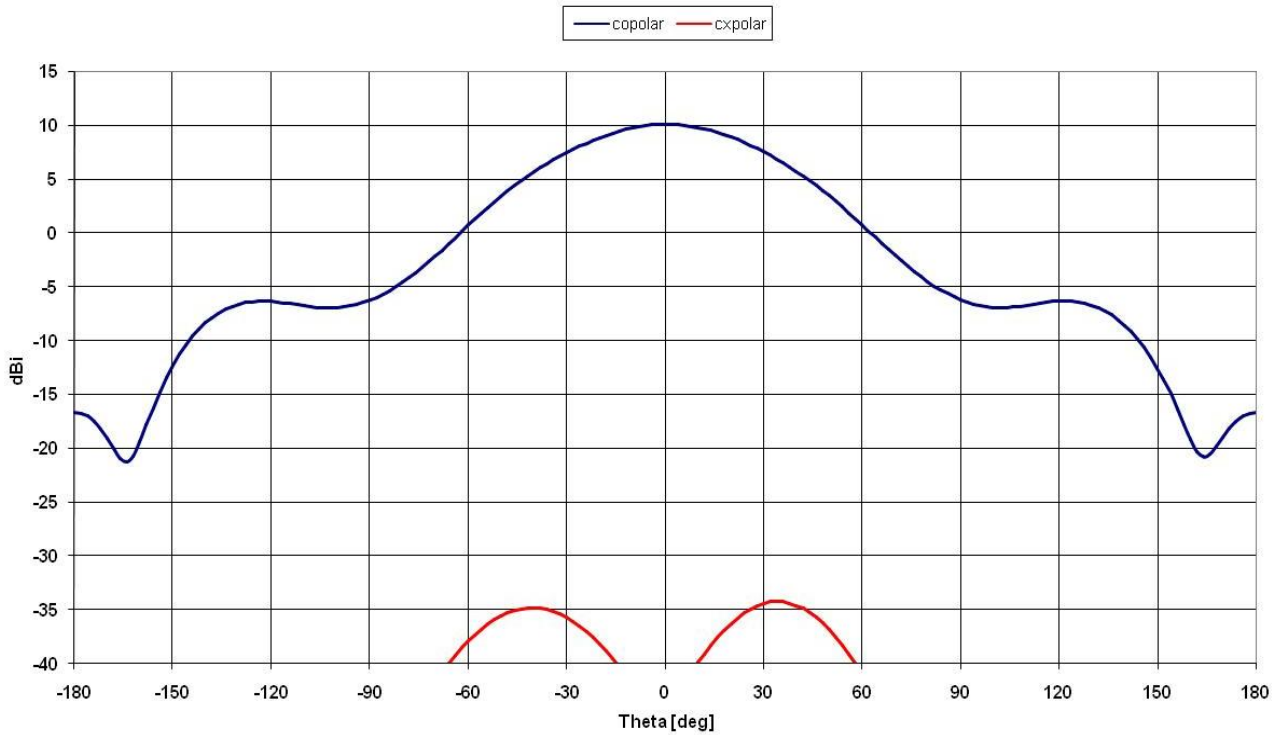


**Figure 4-18:** Directivity pattern @ 1.6 GHz,  $\phi = 90^\circ$ .

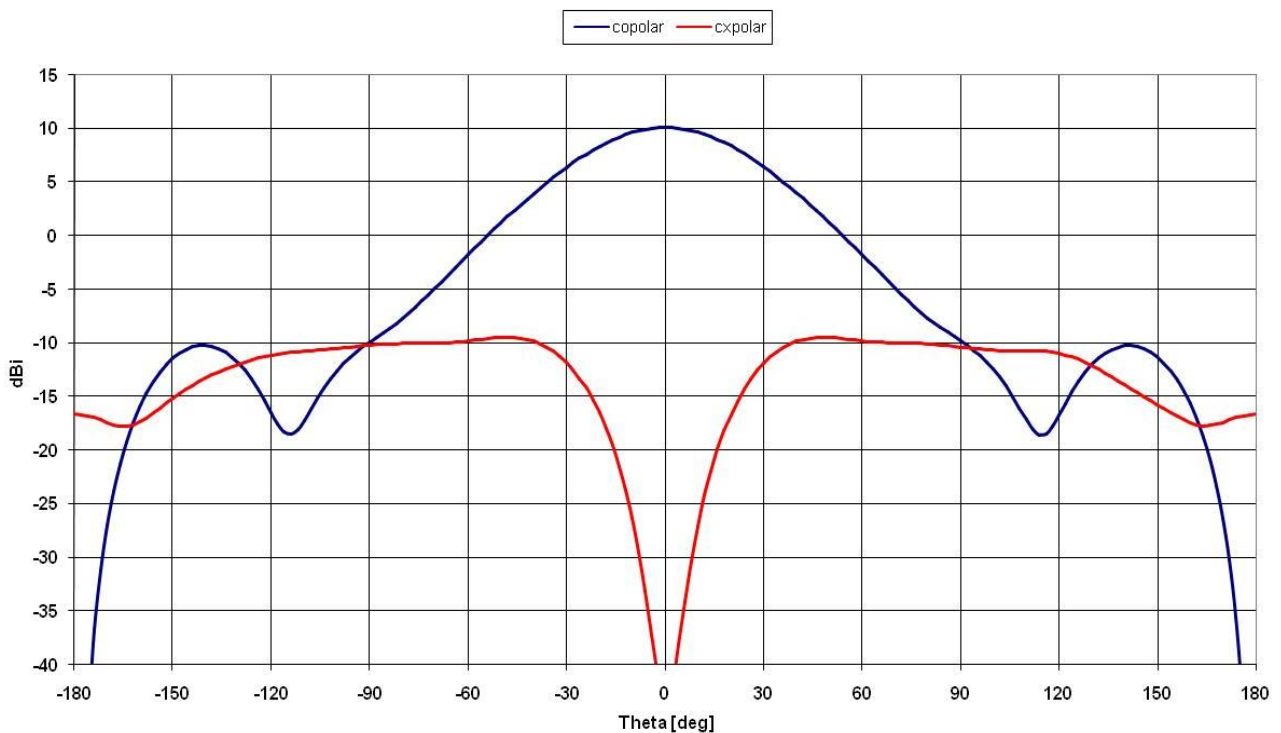


**Figure 4-19:** Directivity pattern @ 1.6 GHz,  $\phi = 135^\circ$ .

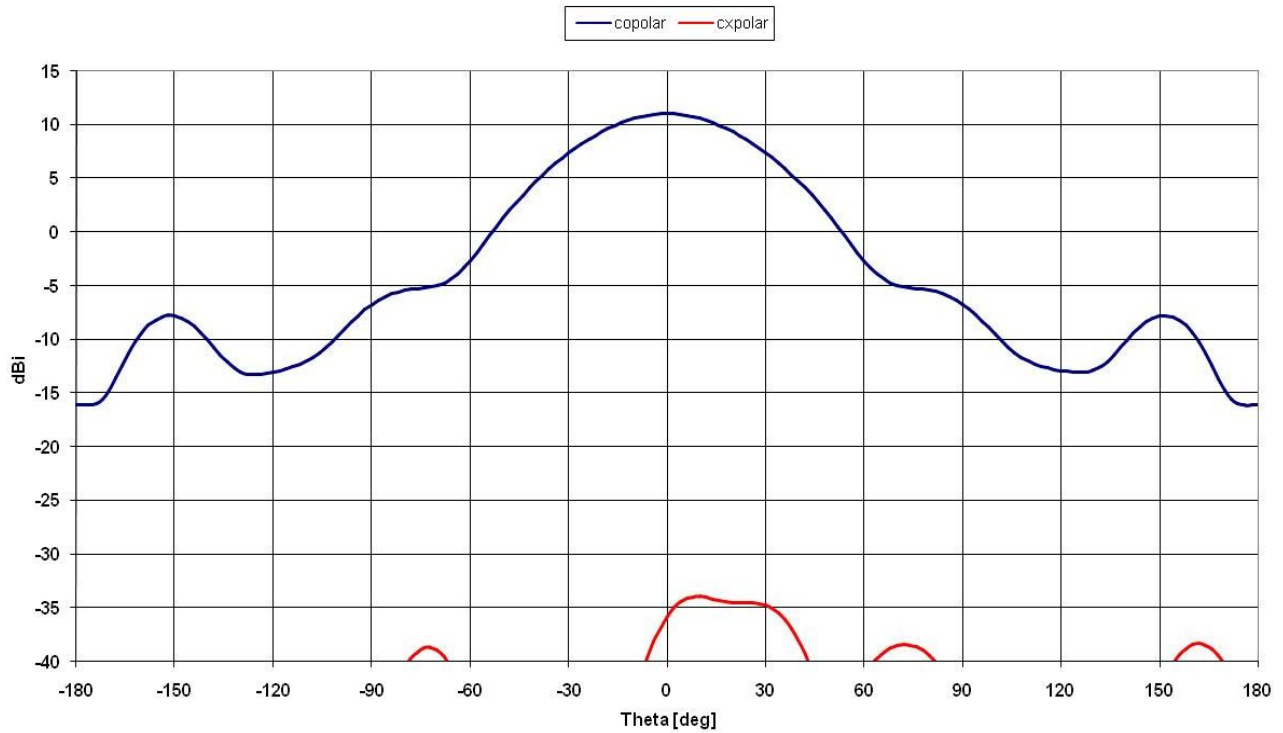


**Figure 4-20:** Directivity pattern @ 2.4 GHz,  $\phi=0^\circ$ .

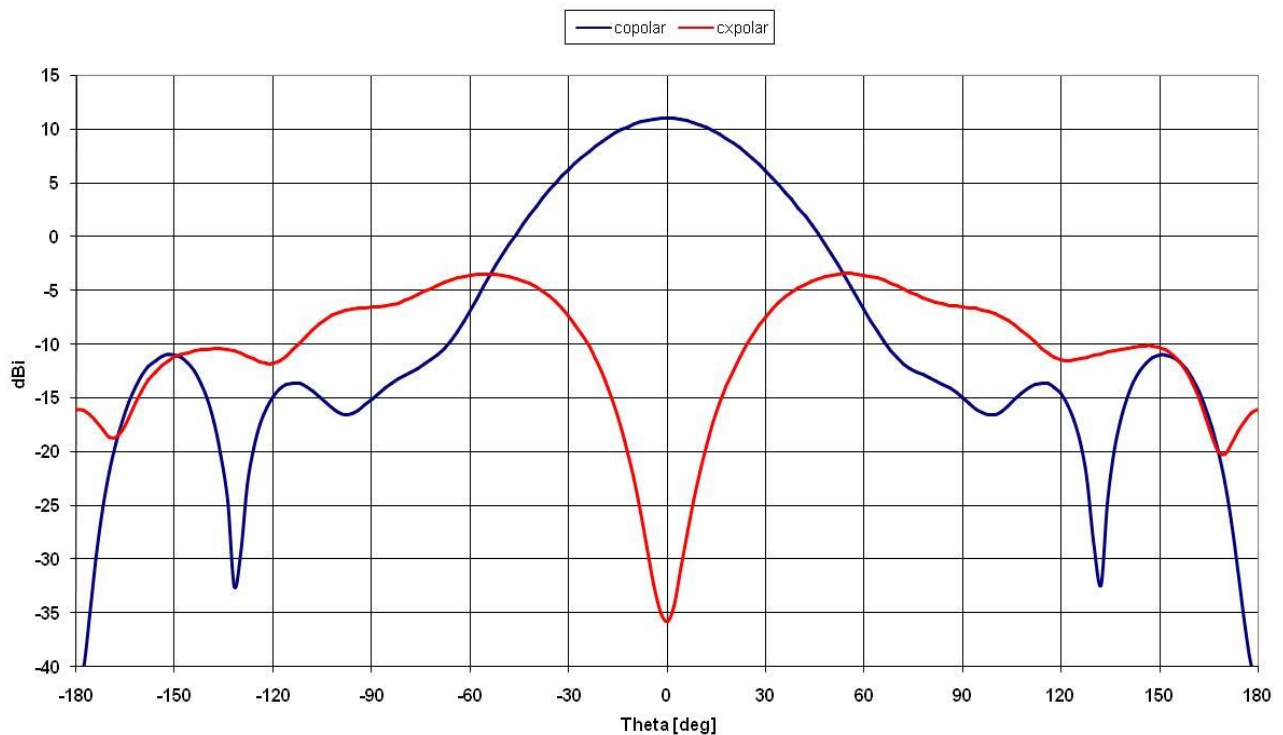


**Figure 4-21:** Directivity pattern @ 2.4 GHz,  $\phi=45^\circ$ .

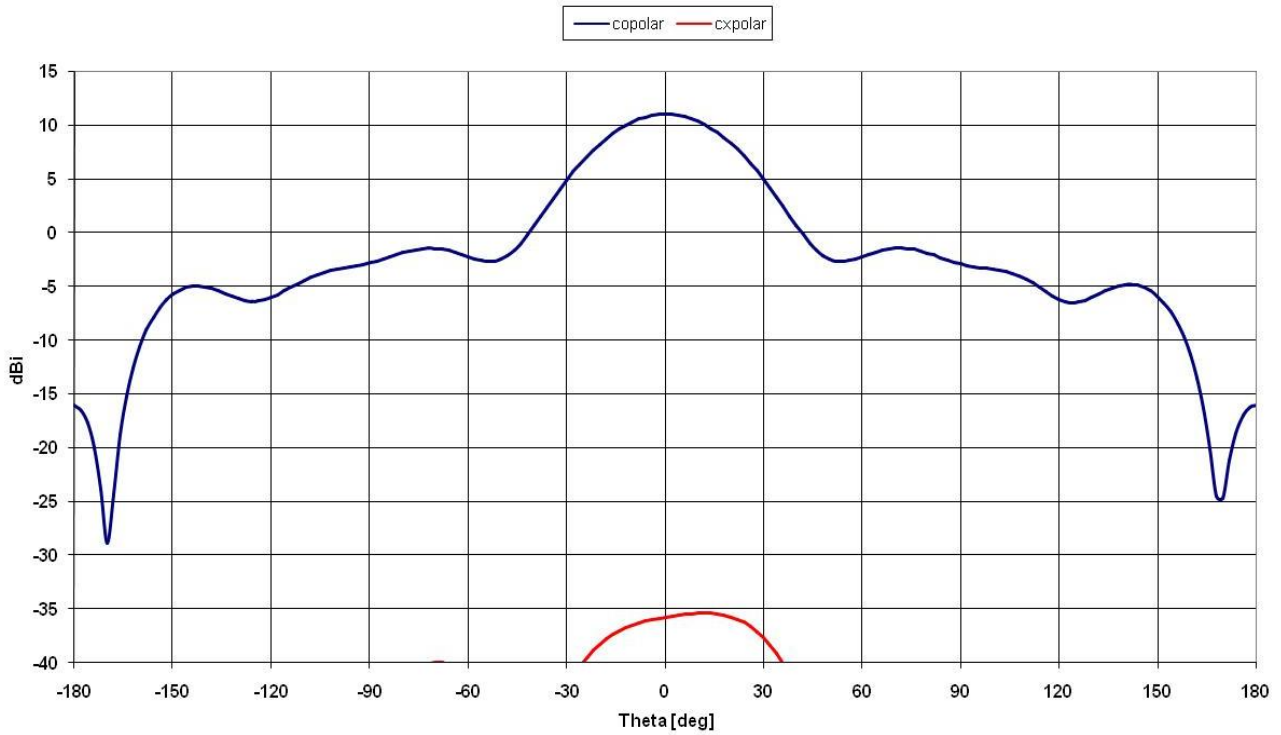


**Figure 4-22:** Directivity pattern @ 2.4 GHz,  $\phi=90^\circ$ .

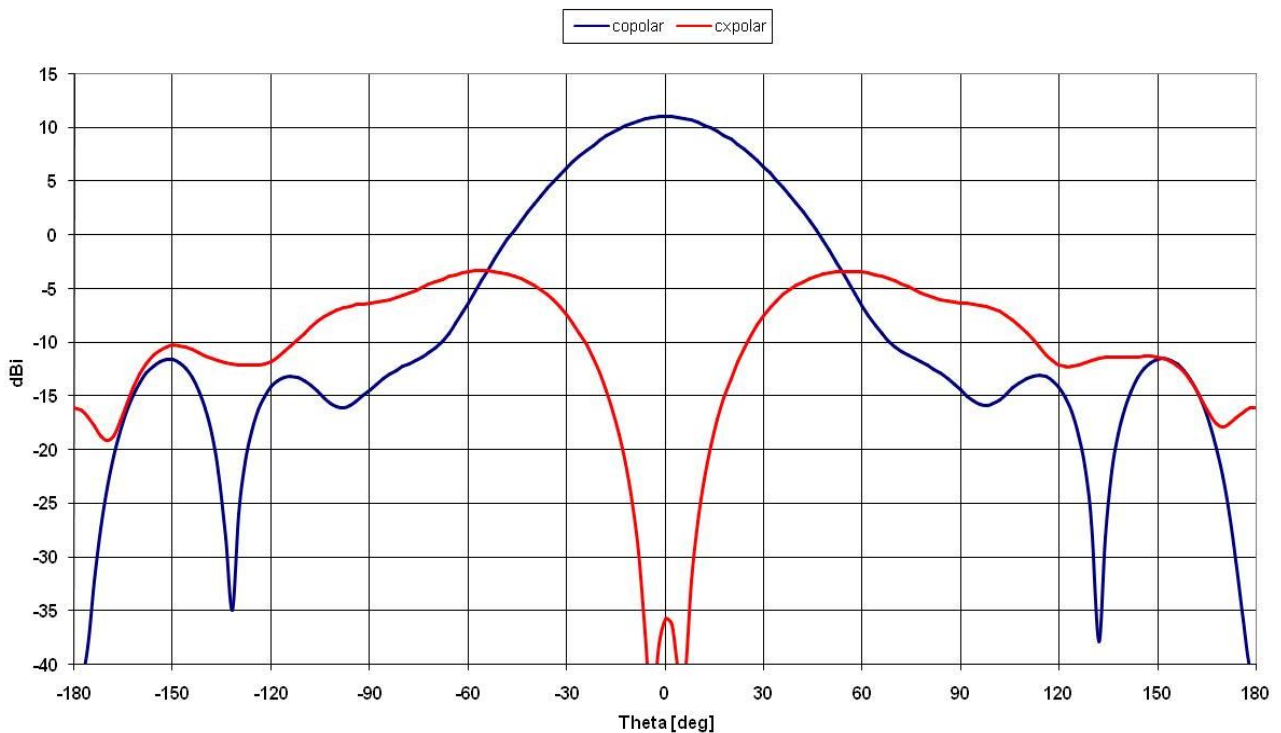


**Figure 4-23:** Directivity pattern @ 2.4 GHz,  $\phi=135^\circ$ .

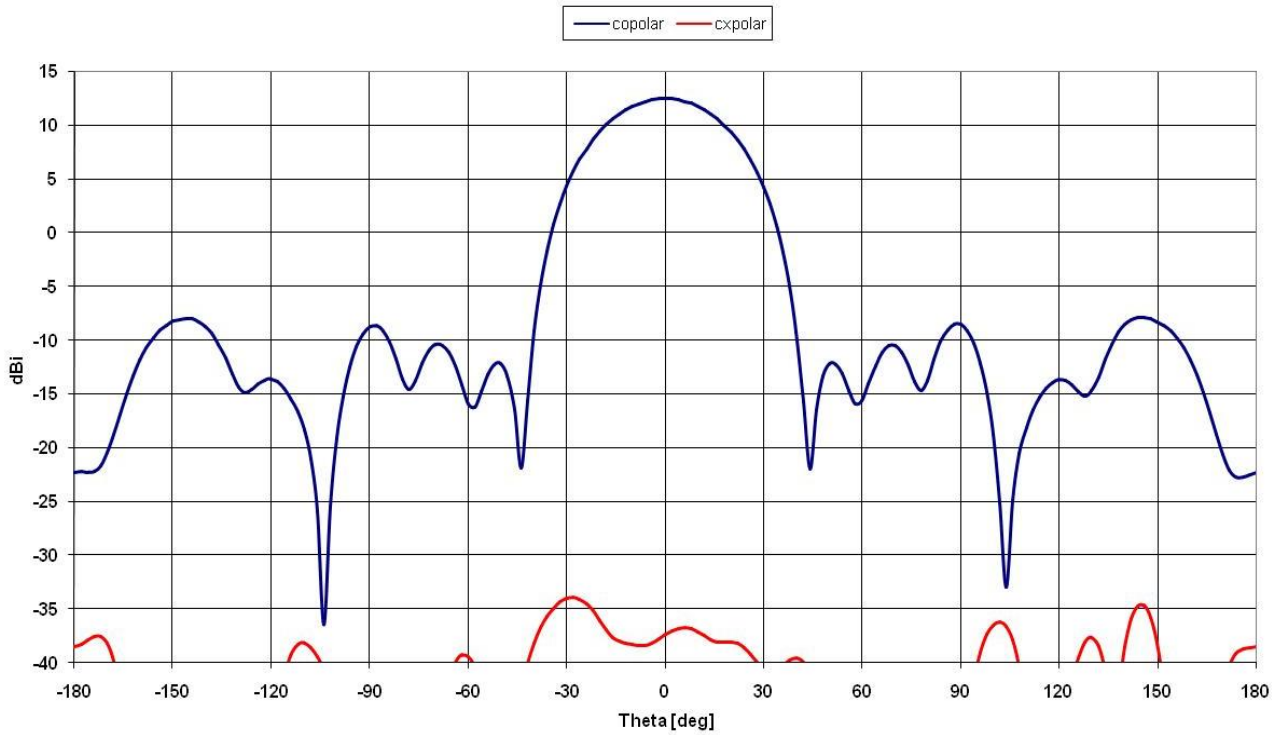


**Figure 4-24:** Directivity pattern @ 5 GHz,  $\phi=0^\circ$ .

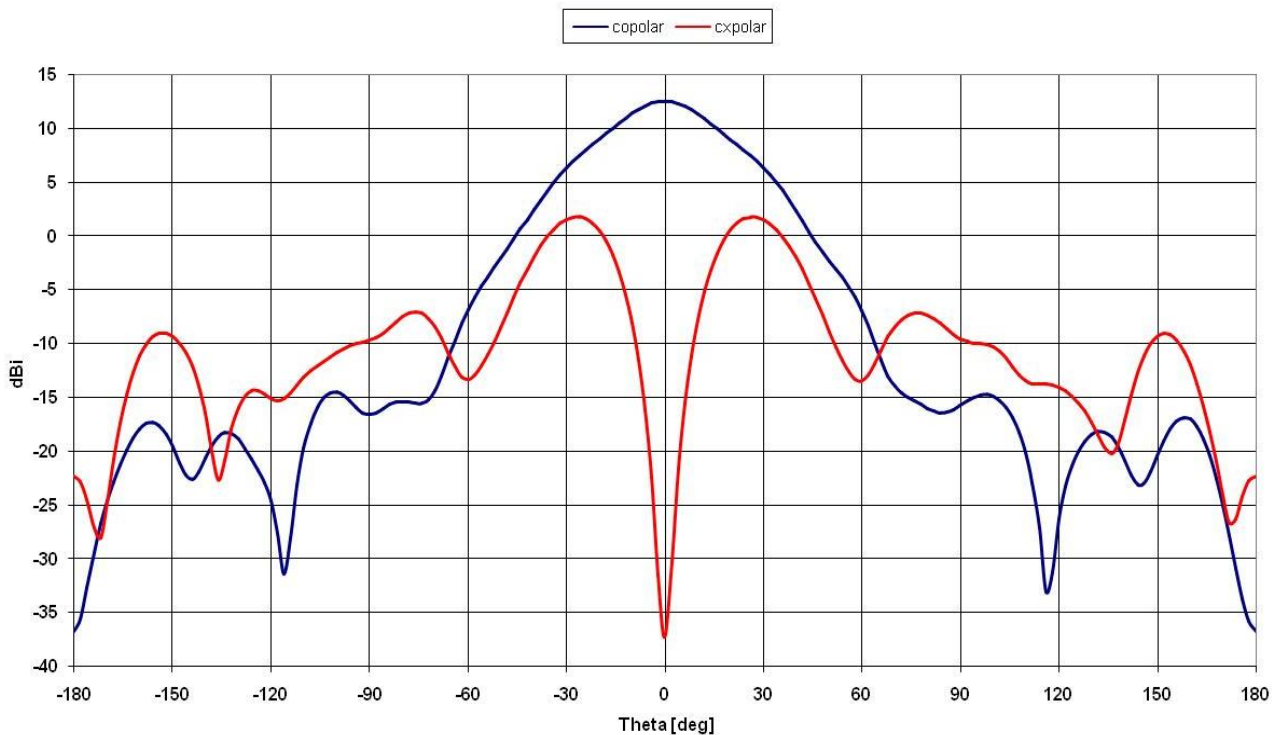


**Figure 4-25:** Directivity pattern @ 5 GHz,  $\phi=45^\circ$ .

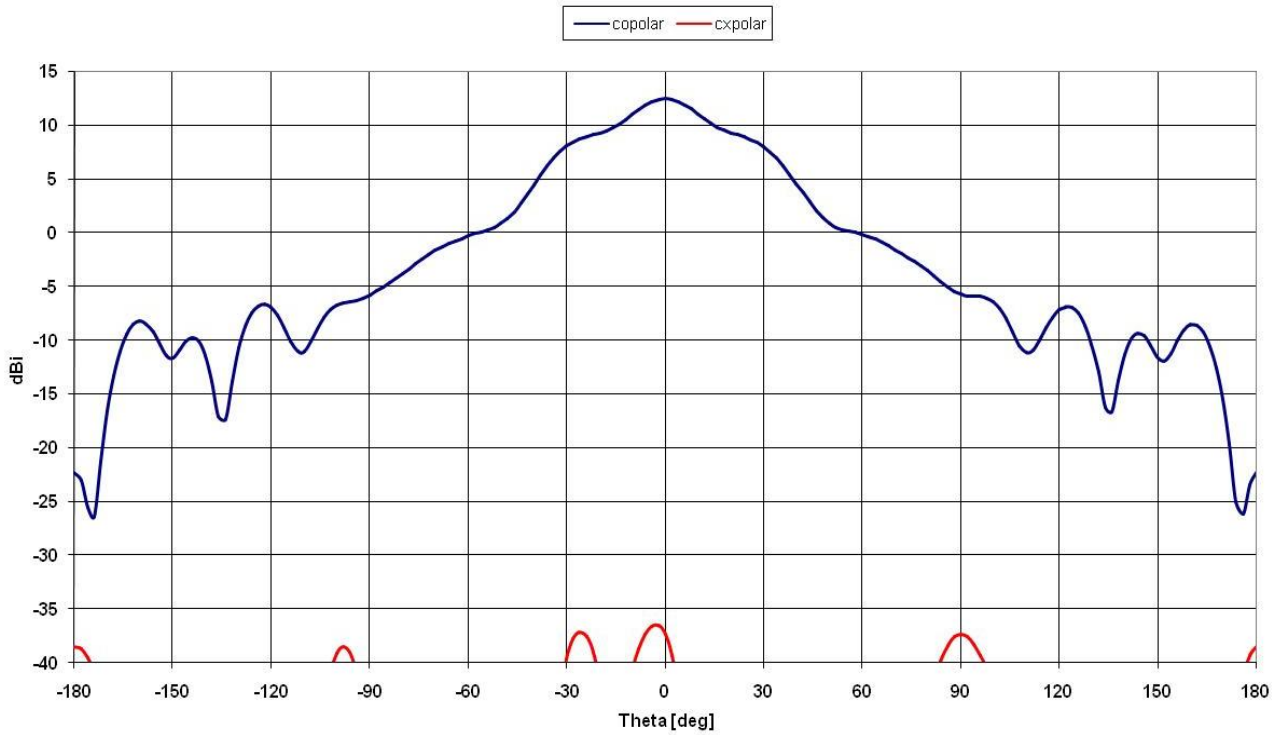


**Figure 4-26:** Directivity pattern @ 5 GHz,  $\phi = 90^\circ$ .

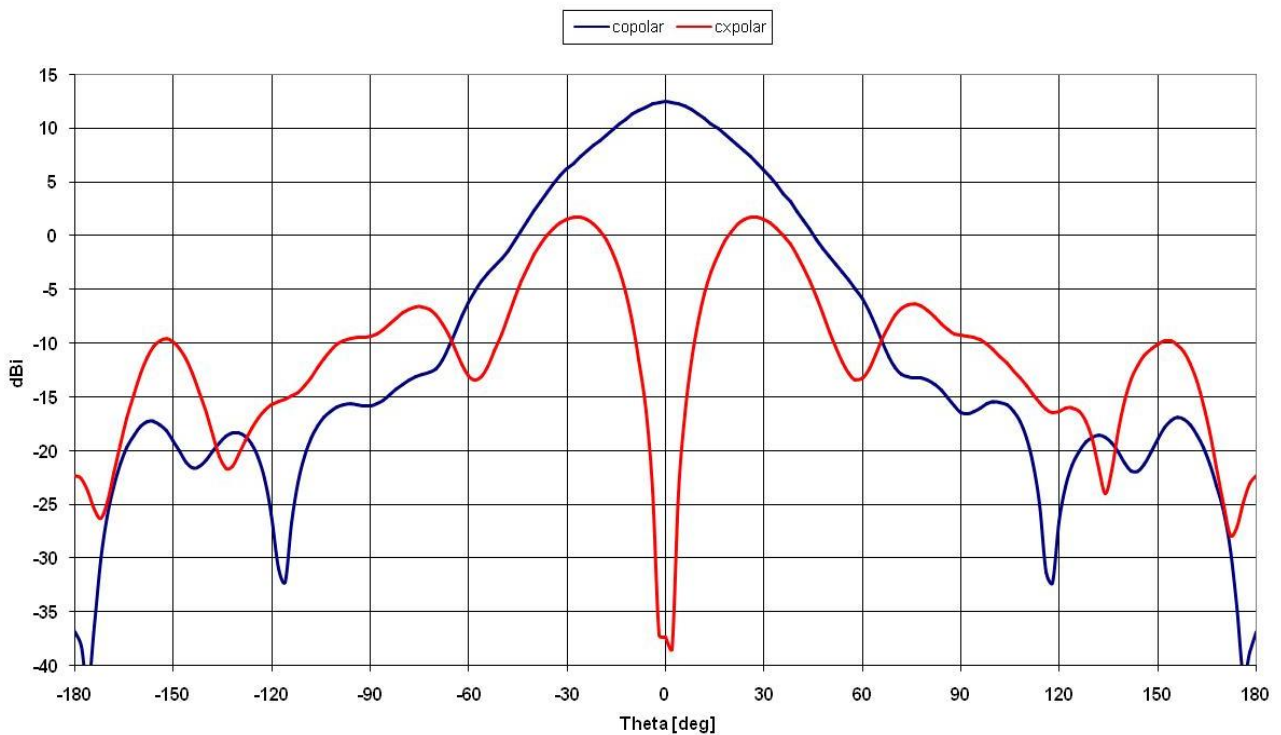


**Figure 4-27:** Directivity pattern @ 5 GHz,  $\phi = 135^\circ$ .



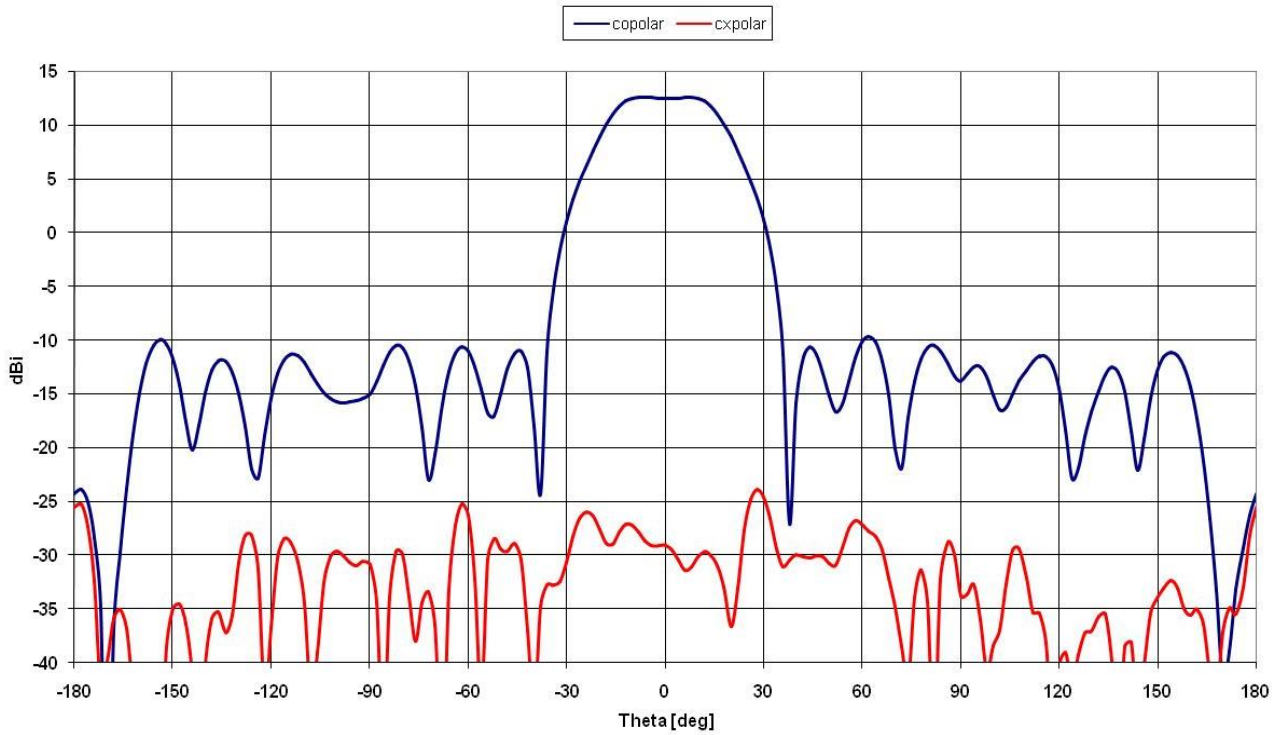


**Figure 4-28:** Directivity pattern @ 6 GHz,  $\phi = 0^\circ$ .

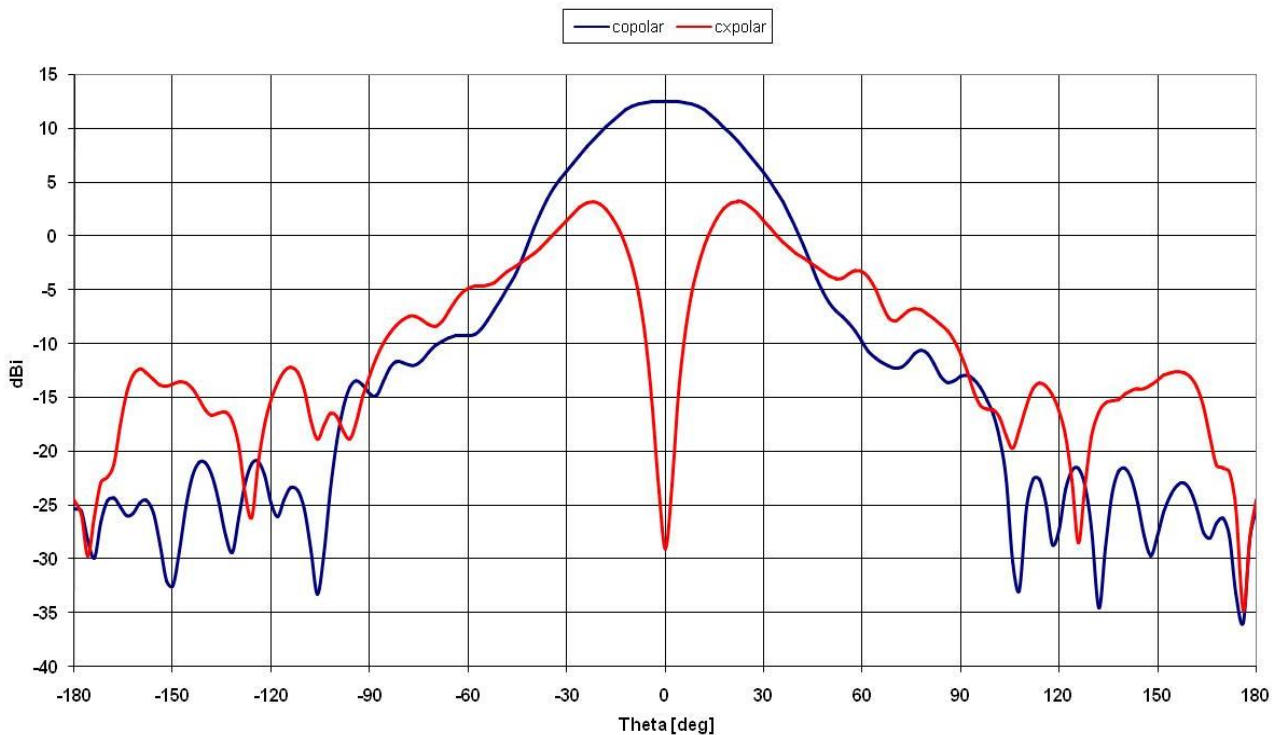


**Figure 4-29:** Directivity pattern @ 6 GHz,  $\phi = 45^\circ$ .

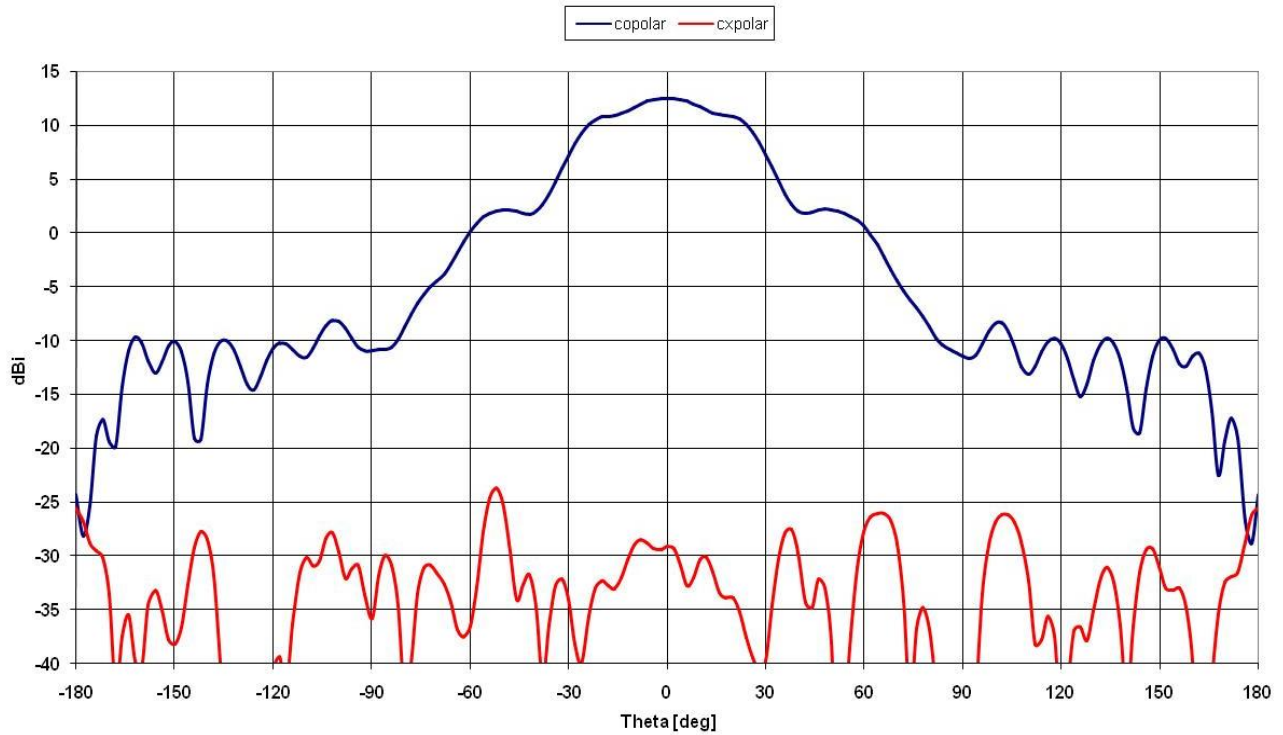


**Figure 4-30:** Directivity pattern @ 6 GHz,  $\phi = 90^\circ$ .

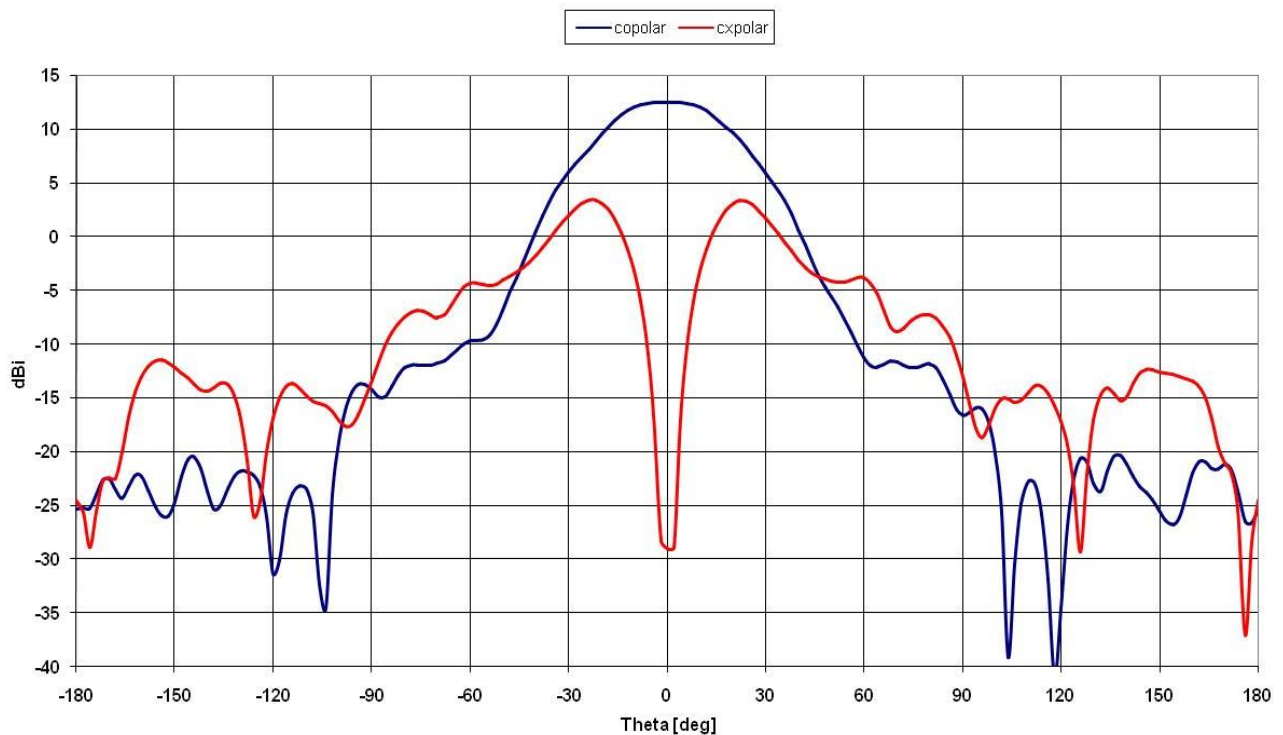


**Figure 4-31:** Directivity pattern @ 6 GHz,  $\phi = 135^\circ$ .



## 5 TYPICAL AND MEASURED DATA ACCURACY

Each SATIMO horn is supplied with measured data on return loss, boresight gain, efficiency and directivity pattern cuts.

### 5.1 RETURN LOSS

The return loss performance of each horn is measured in a suitable anechoic chamber in normal ambient conditions using an Agilent Vector Network Analyzer. A block diagram of the test set-up is shown in Figure 5-1. The accuracy of the calibration data is  $\pm 0.05$  dB @  $-0.5$  dB levels and  $\pm 1$  dB @  $-30$  dB levels.

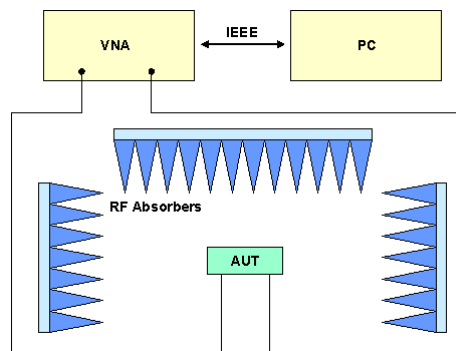


**Figure 5-1:** Block diagram of the test set-up for S-parameters measurements.

### 5.2 BORESIGHT GAIN

The boresight gain data supplied with each horn are typical values for a number of horns calibrated by SATIMO in the SATIMO Multi Probe spherical near field System (SG64) using high accuracy reference antenna and comparison with third party calibrations. The stipulated values include spherical wave low pass filtering with modes equivalent to  $> 99.8$  power percentage. The accuracy of the boresight gain data is  $\pm 0.7$  dB including manufacturing uncertainties.

### 5.3 EFFICIENCY

The horn efficiency data supplied with each horn are typical values for a number of horns calibrated by SATIMO in the SATIMO Multi Probe spherical near field System (SG64) using high accuracy reference antenna and comparison with third party calibrations. The accuracy of the efficiency data is  $\pm 0.5$  dB including manufacturing uncertainties.